



# Diagnosis AI : Advancing Disease Detection Using Artificial Intelligence

**GitHub Repository:** Diagnosis AI

DA526 - Image Processing with Machine Learning  
Project Report

**Team Name:** Image Architects

## Team Members:

Name : Amiya Ghosh	Roll Number: 244161001
Name : Prateek Goel	Roll Number: 244161005
Name : Bishal Sarkar	Roll Number: 244161003
Name : Krishnapal Yadav	Roll Number: 244161016
Name : Tsring Wangchu	Roll Number: 244161007

Instructor:

Dr. Debanga Raj Neog

# Contents

<b>Abstract</b>	<b>1</b>
<b>1 Introduction</b>	<b>2</b>
<b>2 Datasets</b>	<b>3</b>
2.1 Brain Tumor . . . . .	3
2.2 Skin Cancer . . . . .	3
2.3 Pneumonia . . . . .	3
2.4 Lung Cancer . . . . .	4
<b>3 Image and data processing</b>	<b>5</b>
3.1 Brain Tumor . . . . .	5
3.2 Skin cancer . . . . .	5
3.3 Pneumonia . . . . .	6
3.4 Lung Cancer . . . . .	6
<b>4 Model Architectures for Each Disease</b>	<b>7</b>
4.1 Brain Tumor . . . . .	7
4.2 Skin Cancer . . . . .	8
4.3 Pneumonia . . . . .	10
4.4 Lung Cancer . . . . .	11
<b>5 Experiments and Results</b>	<b>13</b>
5.1 Brain Tumor Detection . . . . .	13
5.2 Skin Cancer . . . . .	14
5.3 Pneumonia Detection . . . . .	15
5.4 Lung Cancer Detection . . . . .	17
<b>6 Conclusions</b>	<b>19</b>

# List of Figures

4.1	Architecture of the CNN model for brain tissue classification. . . . .	7
4.2	Architecture using pretrained ResNet50. . . . .	8
4.3	Model Architecture of Skin Cancer Detection . . . . .	9
4.4	Model Architecture of Pneumonia Detection using CNN . . . . .	10
4.5	Model Architecture of Lung Cancer Detection using CNN . . . . .	12
5.1	Results of Model 1 in Brain Tumor Detection . . . . .	14
5.2	Results of Skin cancer Detection Model . . . . .	15
5.3	Results of CNN Architecture in Pneumonia Detection . . . . .	15
5.4	Results of SVM Classifier for Pneumonia Detection . . . . .	16
5.5	Results of Lung Cancer Model . . . . .	18

# List of Tables

5.1	Disease Names and Referred Short Names . . . . .	14
5.2	Results of Skin Cancer Detection . . . . .	14
5.3	Results of CNN Architecture in Pneumonia Detection . . . . .	16
5.4	Results of SVM Classifier in Pneumonia Detection . . . . .	16
5.5	Comparison of SVM and CNN for Chest X-Ray Classification . . . . .	17

# Abstract

## Diagnosis AI: Advancing Disease Detection Using Artificial Intelligence

The Diagnosis AI project aims to develop an AI-powered diagnostic assistant that transforms disease detection. Traditional diagnostic methods often face limitations such as time-consuming procedures, high costs, and risks of human error, which can delay accurate diagnosis and affect patient outcomes. By integrating artificial intelligence (AI) and machine learning (ML), Diagnosis AI automates and enhances diagnostic processes to improve speed, accuracy, and efficiency.

The project utilizes a diverse range of medical image datasets covering brain tumors, nail disorders, lung cancer, breast cancer, and skin cancer. AI models are trained to recognize complex disease patterns and essential diagnostic features. The system's algorithmic framework incorporates advanced image processing techniques combined with Convolutional Neural Networks (CNNs), widely recognized for their strength in analyzing medical images. Transfer learning is applied to improve model efficiency and reduce training time.

To ensure robustness, the project employs image augmentation and explores alternative deep learning architectures such as Region-based CNNs (RCNNs). These approaches enhance the models' adaptability to diverse clinical conditions and mitigate overfitting.

The project culminates in a user-friendly web portal for disease screening, providing fast, accurate assessments for healthcare professionals and patients. This platform demonstrates the real-world impact of AI-driven diagnostics.

In addition to tool development, Diagnosis AI undertakes a comprehensive study of image processing and machine learning techniques for disease detection. Key areas include data selection, preprocessing, model design, and performance evaluation across diseases such as skin cancer, brain tumors, pneumonia, and lung cancer.

Through rigorous performance analysis, the project evaluates model effectiveness, explores clinical implications, and identifies future research opportunities.

Ultimately, Diagnosis AI seeks to transform disease diagnosis, promote early detection, improve patient outcomes, and advance healthcare technology.

# Chapter 1

## Introduction

The field of medical diagnostics is poised at the threshold of a transformative era, driven by rapid advancements in image processing, machine learning, and artificial intelligence (AI). The early detection of critical diseases—including skin cancer, brain tumors, pneumonia, and lung cancer—is paramount, as timely diagnosis significantly enhances treatment effectiveness and improves patient survival rates. Despite the progress in conventional diagnostic methods, challenges such as variability in human interpretation, time constraints, and the complexity of medical data persist. To address these limitations, this project seeks to harness the power of large-scale medical imaging datasets combined with advanced computational algorithms.

By integrating cutting-edge techniques in deep learning, particularly Convolutional Neural Networks (CNNs), and employing robust image processing strategies, the project aims to design, develop, and rigorously evaluate AI-driven diagnostic models capable of accurately identifying disease-specific patterns and features. The initiative emphasizes not only the development of predictive models but also the systematic assessment of their performance, generalizability, and clinical relevance across diverse medical imaging modalities.

Through this interdisciplinary approach, the project aspires to contribute to the growing body of research that underscores the transformative potential of AI in healthcare. Ultimately, the goal is to create diagnostic tools that support clinicians in making faster, more accurate decisions, thereby advancing patient care and improving health outcomes on a broader scale.

# **Chapter 2**

## **Datasets**

### **2.1 Brain Tumor**

The Brain MRI Images dataset consists of 253 brain MRI scans, organized into two categories: “yes” and “no.” The “yes” category includes 155 images depicting cases with brain tumors, while the “no” category contains 98 images representing non-tumorous cases. This dataset offers valuable insights into the varied manifestations of brain tumors and serves as a critical resource for developing and training accurate diagnostic models.

Data : Brain MRI Images for Brain Tumor Detection Dataset

### **2.2 Skin Cancer**

The HAM10000 dataset underpins the skin cancer detection models in this project. It contains 10,015 dermatoscopic images spanning seven diagnostic categories: actinic keratoses (akiec), basal cell carcinoma (bcc), benign keratosis-like lesions (bkl), dermatofibroma (df), melanoma (mel), melanocytic nevi (nv), and vascular lesions (vasc). Over half of the cases are confirmed via histopathology, with others verified through follow-up exams, expert consensus, or in-vivo confocal microscopy.

Data : Skin Cancer MNIST: HAM10000 Dataset

### **2.3 Pneumonia**

The dataset is structured into three folders (train, test, validation) with subfolders for each category (Pneumonia and Normal). It comprises 5,863 chest X-ray images collected from pediatric patients aged one to five years at Guangzhou Women and Children’s Medical Center. All X-rays were obtained during routine clinical care. For quality assurance, low-quality or unreadable scans were removed before

analysis. Data : Chest X-ray Pneumonia Dataset

## 2.4 Lung Cancer

Chest X-ray images form the foundation for the lung cancer classification models in this project. The dataset includes images representing various lung cancer subtypes, including adenocarcinoma, large cell carcinoma, squamous cell carcinoma, as well as normal cases. This diverse collection provides a comprehensive view of lung cancer pathology, supporting the development of robust models capable of accurately identifying and classifying different subtypes.

By leveraging these rich and varied medical imaging datasets, the project applies advanced image processing and machine learning techniques to develop accurate, reliable diagnostic models for skin cancer, brain tumors, pneumonia, and lung cancer. Data : IQ-OTH/NCCD Lung Cancer Dataset

# **Chapter 3**

## **Image and data processing**

### **3.1 Brain Tumor**

Image preprocessing for brain tumor detection involves a sequence of steps specifically designed for MRI images:

- Convert the input image from BGR to grayscale to simplify its representation and highlight key features.
- Apply a Gaussian blur with a kernel size of (5x5) and a standard deviation of 0 to reduce image noise and improve clarity.
- Perform binary thresholding with a threshold value of 45 to separate the brain region from the background.
- Apply two iterations of erosion followed by two iterations of dilation to enhance the quality of the segmented brain region.
- Detect contours in the thresholded image to identify the boundaries of the brain.
- Select the contour with the largest area, corresponding to the primary brain region of interest.
- Determine the extreme points (leftmost, rightmost, topmost, and bottommost) to define a bounding box around the brain.
- Crop the original image using the bounding box to isolate the brain region.
- Output the cropped image containing only the brain region for further analysis.

### **3.2 Skin cancer**

Image preprocessing for skin cancer involves multiple steps to enhance image quality and standardize inputs for analysis:

- Resize all images to a uniform size, typically 28x28 pixels, ensuring consistency and compatibility with the model architecture.

- Normalize pixel values to a common scale, usually between 0 and 1, to support efficient model training and convergence.
- Apply augmentation techniques—including rotation, flipping, and zooming—to increase the diversity of the training dataset and improve model generalization.
- Address class imbalance by applying oversampling methods to ensure balanced representation across diagnostic categories.
- Divide the dataset into training and testing sets to facilitate model training and performance evaluation.

### 3.3 Pneumonia

- Accepts images of size 64x64 with 3 color channels (RGB).
- Applies 32 filters of size 3x3, producing a feature map of shape (32, 32, 32).
- Reduces spatial dimensions to (16, 16, 64) by downsampling the feature map.
- Applies 128 filters of size 3x3, resulting in a feature map of (8, 8, 128).
- Converts the 3D feature maps into a 1D vector of length 8192 for dense layer processing.
- Contains 1 neuron, likely representing the output unit for binary classification (Pneumonia vs Normal).
- Additional fully connected layer to enhance learning capacity (exact number of neurons not specified).

### 3.4 Lung Cancer

Image preprocessing for lung cancer detection focuses on standardizing the images and preparing them for model input:

- Resize images to a fixed size to ensure uniformity and compatibility with the model architecture.
- Convert images to grayscale to simplify the representation and reduce computational complexity.
- Normalize pixel values to a common scale, typically ranging from 0 to 1, to facilitate model training and convergence.
- Split the dataset into training, validation, and testing sets for model training, validation, and evaluation, respectively.
- Apply data augmentation (rotation, flipping, zooming) to improve dataset diversity and model robustness.

# Chapter 4

## Model Architectures for Each Disease

### 4.1 Brain Tumor

#### Model 1

- Input layer accepts 240x240 pixel RGB images.
- Zero-padding preserves spatial information.
- Conv layer with 32 filters (7x7) extracts key features.
- Batch normalization stabilizes training.
- ReLU activation adds non-linearity.
- Two max-pooling layers reduce spatial dimensions.
- Output is flattened.
- Fully connected layer with sigmoid activation outputs brain tissue probability.
- Optimized for binary brain tissue classification.

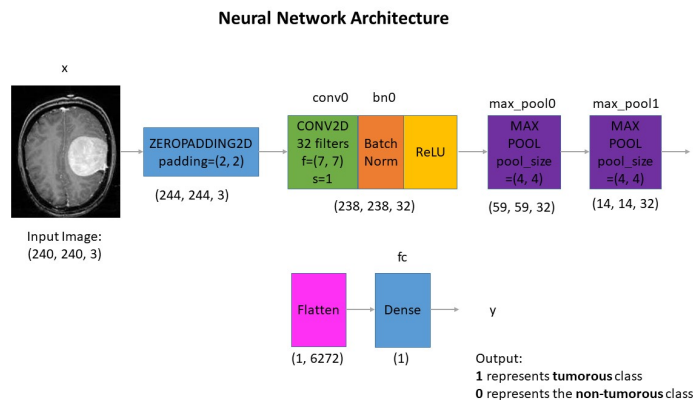


Figure 4.1: Architecture of the CNN model for brain tissue classification.

## Model 2

- The model uses a pre-trained ResNet50 base to process input images of 240x240 pixels with three color channels (RGB).
- The base model's layers are frozen to retain previously learned representations.
- A global average pooling layer reduces the spatial dimensions of the feature maps.
- A dense layer with ReLU activation performs further feature extraction.
- The output layer uses sigmoid activation to predict the probability of brain tumor presence.
- The model is compiled with the Adam optimizer, binary cross-entropy loss, and accuracy as the evaluation metric.
- Training is conducted for 10 epochs.
- The model's performance is evaluated on a test set.
- The architecture leverages transfer learning for effective brain tumor classification.

## Brain Tumor Classification

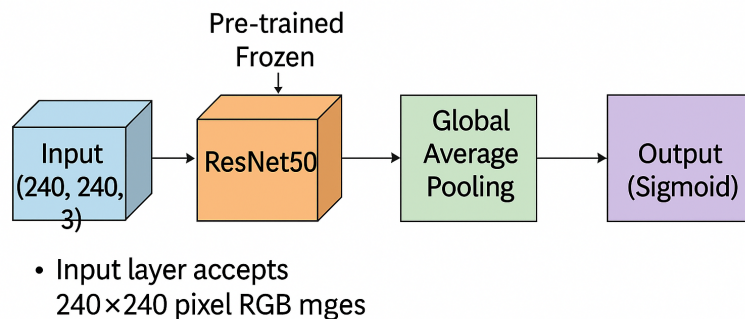


Figure 4.2: Architecture using pretrained ResNet50.

## 4.2 Skin Cancer

- The model processes RGB images of size  $(28 \times 28 \times 3)$  through the input layer.
- Two **convolutional layers** follow, each using **ReLU activation** and padding to maintain spatial dimensions.

- A **max-pooling layer** reduces spatial dimensions by downsampling the feature maps.
- Two additional **convolutional layers** further extract higher-level features.
- Another **max-pooling layer** is applied to further downsample the feature maps.
- The resulting feature maps are **flattened** into a 1D vector.
- The flattened vector passes through **two fully connected dense layers** with **ReLU activation**.
- The **output layer** has **7 units**, corresponding to the skin cancer types, and uses **softmax activation** for multiclass classification.
- This hierarchical structure allows the model to learn and integrate features at multiple levels of abstraction for accurate skin cancer classification.

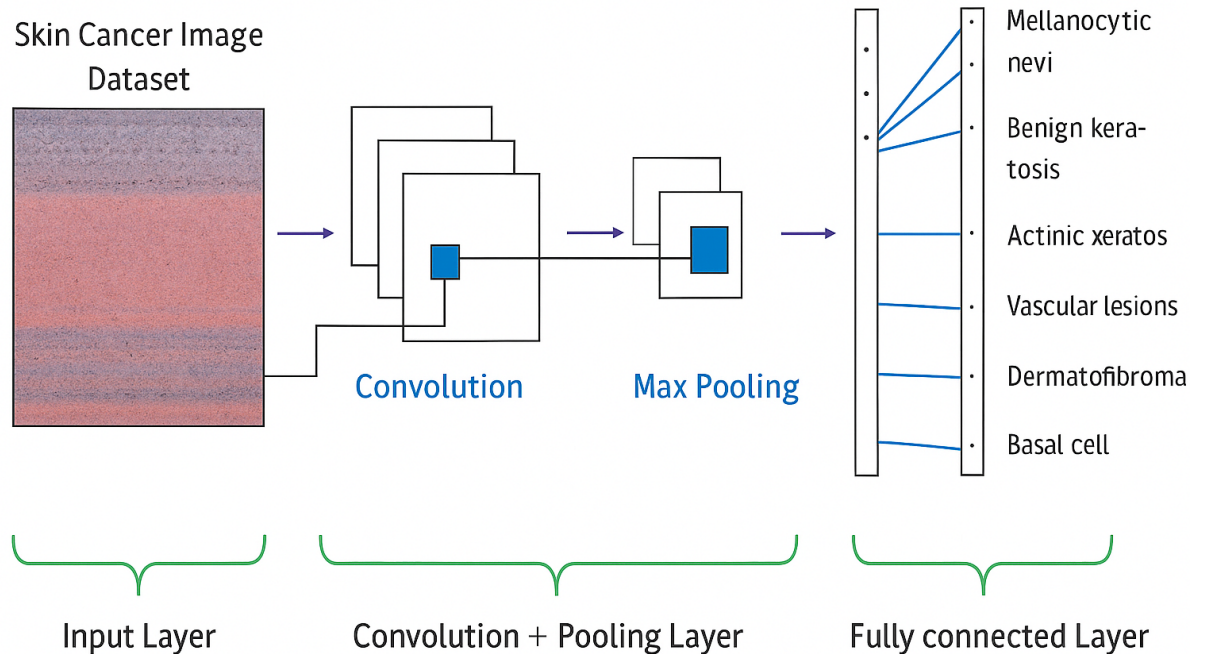


Figure 4.3: Model Architecture of Skin Cancer Detection

## 4.3 Pneumonia

### Model 1 : CNN Architecture

#### Model Development

**Architecture:** The CNN model architecture comprises a series of convolutional layers followed by max-pooling operations to extract features and reduce spatial dimensions. The initial convolutional layer, conv2d\_2, processes the input data with 32 filters, resulting in an output shape of (148, 148, 32). Subsequent max-pooling reduces the spatial dimensions by half. The following conv2d\_4 layer applies 64 filters to the feature maps, producing an output shape of (72, 72, 64), which is again downsampled by max-pooling. The pattern continues with conv2d\_4\_2, which increases the filter count to 128, resulting in an output shape of (34, 34, 128). After another max-pooling operation, conv2d\_3 further processes the features with 128 filters, resulting in an output shape of (15, 15, 128). Finally, the feature maps are flattened to a vector representation and fed into two fully connected dense layers with 512 and 1 units, respectively, for classification. The total number of parameters in the model architecture is 3,452,545.

**Hyperparameter Tuning:** Random Search from Keras Tuner optimized the model's hyperparameters.

**Training:** The best hyperparameter settings trained the model for 50 epochs, ensuring sufficient learning without overfitting.

#### Hyperparameter Tuning Details

- Filters in convolutional layers varied from 32 to 128.
- Kernel sizes for convolutional layers were 3x3 and 5x5.
- Dense layer units ranged from 32 to 512.
- Learning rates tested were 1e-2, 1e-3, and 1e-4.

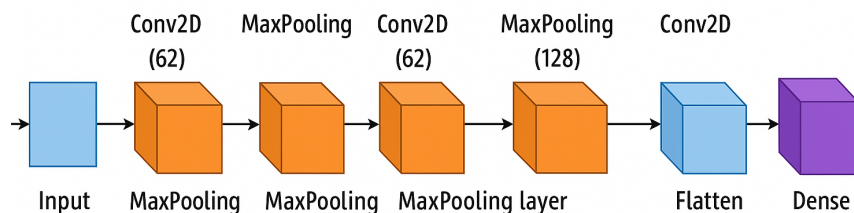


Figure 4.4: Model Architecture of Pneumonia Detection using CNN

## Model 2 : SVM Classifier

### Model Specifications

- **Model Type:** Support Vector Machine (SVM)
- **Kernel Type:** Linear
- **Feature Descriptor:** Histogram of Oriented Gradients (HOG)
- **Image Dimensions (for HOG):** 150 x 150 pixels

### Feature Extraction Parameters

- Orientations: 8
- Pixels per Cell: (16, 16)
- Cells per Block: (1, 1)
- Block Normalization: L2-Hys

## 4.4 Lung Cancer

The following is the CNN Architecture for the Lung Cancer detection model

- **Input Layer:** Accepts images of size (64, 64, 3).
- **Convolutional Layers:** Three convolutional layers with increasing filter sizes (16, 32, and 64) and ReLU activation.
- **Max Pooling Layers:** Downsample the feature maps.
- **Flatten Layer:** Transitions from convolutional layers to fully connected dense layers.
- **Dense Layers:** Three dense layers with 256, 128, and 64 units, respectively, using ReLU activation.
- **Output Layer:** Softmax activation for multiclass classification.

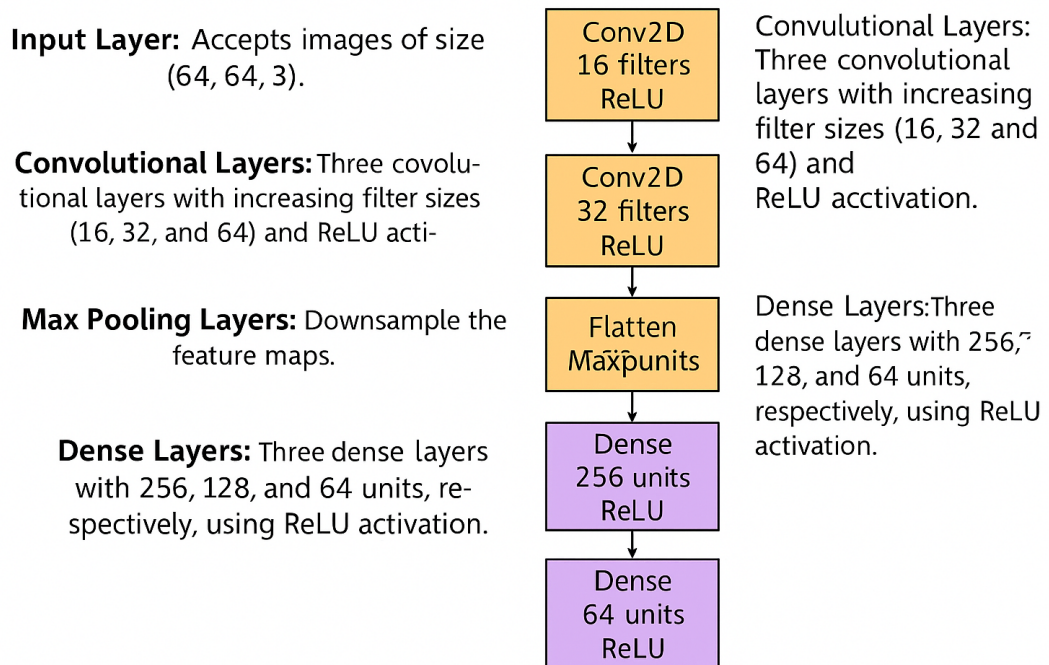


Figure 4.5: Model Architecture of Lung Cancer Detection using CNN

# Chapter 5

## Experiments and Results

### 5.1 Brain Tumor Detection

#### Model 1

The model achieved promising results in the task of binary brain tumor detection. With a total of 11,137 parameters, of which 11,073 are trainable, the model demonstrates its ability to effectively learn and extract relevant features from input images. Utilizing the Adam optimizer and binary cross-entropy loss function, the model underwent training for 24 epochs. On the test dataset, the model attained a test loss of 0.24 and a test accuracy of 91%, indicating its robustness in classifying brain tumor images. Furthermore, the model's performance was evaluated on both the validation and test sets, resulting in accuracies of 91% and 89%, respectively. Additionally, the F1 scores for the validation and test sets were calculated at 0.91 and 0.88, demonstrating the model's balanced precision and recall.

#### Model 2

The model, equipped with a total of 24,112,513 parameters, of which 524,801 are trainable, showcased its performance in binary classification for brain tumor detection. Employing the Adam optimizer and binary cross-entropy loss function, the model underwent rigorous training. Upon evaluation, the model achieved a test accuracy of 62.47% with a corresponding test loss of 0.6471, indicating moderate performance on unseen data. The model's validation and test accuracies were 71% and 72%, respectively. F1 scores for both validation and test sets were 71% and 72%.

**Model 1**

	Validation	Test
Accuracy	91%	89%
F1 Score	0.91	0.88

**Model 2**

	Validation	Test
Accuracy	71%	72%
F1 Score	71%	72%

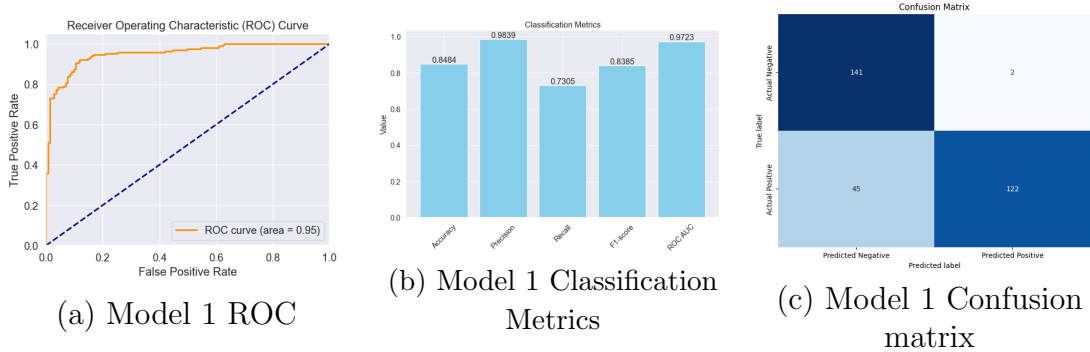


Figure 5.1: Results of Model 1 in Brain Tumor Detection

## 5.2 Skin Cancer

Table 5.1: Disease Names and Referred Short Names

Disease Name	Short Name
Melanocytic Nevi	nv
Melanoma	mel
Benign Keratosis-like Lesions	bkl
Basal Cell Carcinoma	bcc
Pyogenic Granulomas and Hemorrhage	vasc
Actinic Keratoses and Intraepithelial Carcinoma	akiec
Dermatofibroma	df

Table 5.2: Results of Skin Cancer Detection

Class	Precision	Recall	F1 Score	Support
akiec	0.97	1.00	0.99	1339
bcc	0.99	0.99	0.99	1318
bkl	0.94	0.97	0.96	1292
df	0.99	1.00	1.00	1351
nv	0.89	0.88	0.88	1374
vasc	1.00	1.00	1.00	1335
mel	0.95	0.91	0.93	1365
<b>Accuracy</b>				0.96 9387

The skin cancer detection model achieves an impressive accuracy of 96%, demonstrating its effectiveness in classifying dermatoscopic images into seven diagnostic categories. The precision, recall, and F1-score values are high across all classes, indicating reliable performance in identifying various types of skin lesions.

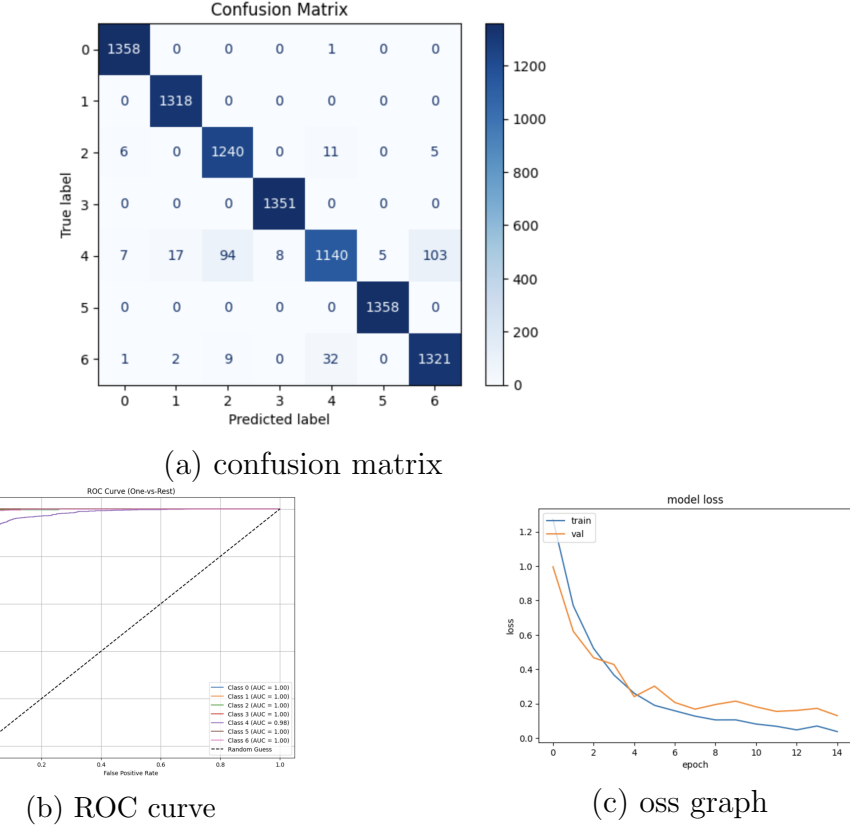


Figure 5.2: Results of Skin cancer Detection Model

## 5.3 Pneumonia Detection

### CNN Architecture

#### Model Training Performance

The validation accuracy peaked at 97.39% at epoch 16. F1 scores for each class fluctuated, indicating variability in model performance over epochs. The high recall reflects the model's sensitivity to pneumonia presence, emphasizing the detection of as many positive cases as possible. The implications of the precision-recall trade-off and the potential impact on clinical practice were also examined.

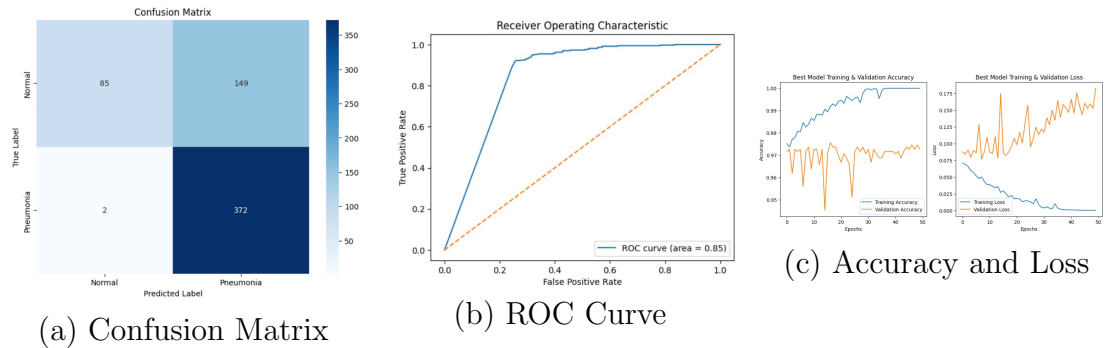


Figure 5.3: Results of CNN Architecture in Pneumonia Detection

Table 5.3: Results of CNN Architecture in Pneumonia Detection

Class	Precision	Recall	F1 Score	Support
0	0.98	0.36	0.53	234
1	0.71	0.99	0.83	374
<b>Accuracy</b>				0.75
<b>Macro Avg</b>	0.85	0.68	0.68	608
<b>Weighted Avg</b>	0.82	0.75	0.72	608

## SVM Classifier

The Support Vector Machine (SVM) classifier was also applied to the pneumonia detection task. In this approach, the images were first resized and converted into grayscale format. Feature extraction was performed using the Histogram of Oriented Gradients (HOG) descriptor, which transformed the images into feature vectors suitable for classification. The SVM classifier was trained using these HOG features with a linear kernel.

Table 5.4: Results of SVM Classifier in Pneumonia Detection

Class	Precision	Recall	F1 Score	Support
0	0.96	0.49	0.65	234
1	0.75	0.99	0.86	374
<b>Accuracy</b>				0.64
<b>Macro Avg</b>	0.86	0.74	0.75	608
<b>Weighted Avg</b>	0.83	0.79	0.77	608

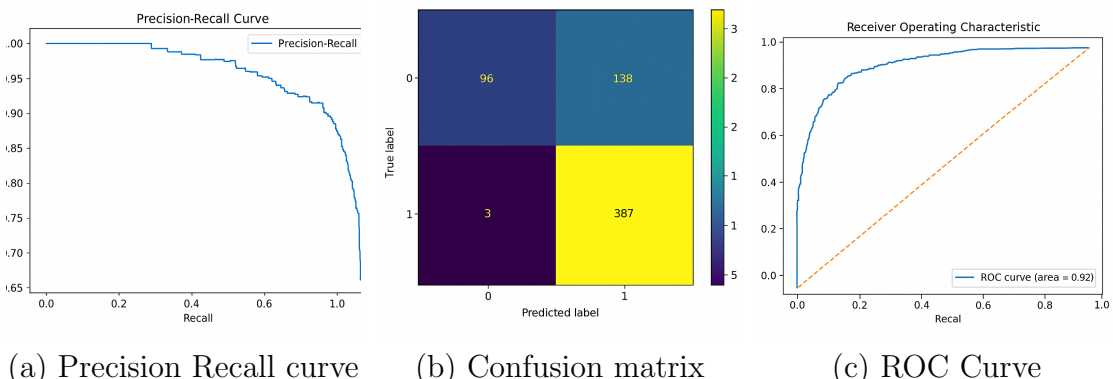


Figure 5.4: Results of SVM Classifier for Pneumonia Detection

### CNN vs. SVM Classifier Comparison

A comparative analysis was conducted to evaluate the performance of the CNN and SVM classifiers for pneumonia detection. The CNN model significantly outperformed the SVM model across all evaluation metrics, including accuracy, precision, recall, and F1-score. The superior performance of the CNN can be attributed to its ability to automatically learn complex features from the raw image data, unlike the SVM classifier, which relies on manually engineered features extracted using the HOG descriptor.

Table 5.5: Comparison of SVM and CNN for Chest X-Ray Classification

Metric	SVM	CNN
Precision (Class 0)	0.97	0.98
Recall (Class 0)	0.41	0.36
F1-Score (Class 0)	0.58	0.53
Support (Class 0)	234.0	234.0
Precision (Class 1)	0.74	0.71
Recall (Class 1)	0.99	0.99
F1-Score (Class 1)	0.85	0.83
Support (Class 1)	390.0	374.0
Accuracy	0.774	0.75
AUC (ROC Curve)	0.92	0.85

Based on the criteria prioritizing the minimization of false negatives (FN), and subsequently false positives (FP) when FNs are equal, the SVM model is recommended. Both SVM and CNN demonstrate a high recall for pneumonia (Class 1) at 0.99, indicating excellent ability to identify positive pneumonia cases. However, considering false positives as the secondary criterion, the SVM model outperforms CNN, with fewer false positives (138 vs. 149). This suggests SVM is less likely to incorrectly classify normal cases as pneumonia—an important advantage in clinical settings where false alarms can have significant consequences. Additionally, SVM exhibits a slightly higher overall accuracy (0.774) and a superior AUC (0.92) compared to CNN's accuracy (0.75) and AUC (0.85). These factors highlight SVM's balanced performance in both sensitivity and specificity, providing strong justification for its recommendation for this classification task.

## 5.4 Lung Cancer Detection

The lung cancer detection model achieved an accuracy of 51% on the test dataset, accompanied by an Area Under the Curve (AUC) value of 0.76. While these re-

sults indicate a degree of predictive capability, the overall performance remains suboptimal. Several factors contribute to this outcome. Firstly, the dataset exhibits a pronounced class imbalance, with significant disparities in the distribution of images across the four lung cancer categories. Such imbalance can bias the model's learning process, making it more challenging to accurately classify under-represented classes. Additionally, the dataset is relatively small, particularly in terms of high-quality, labeled image data. This limitation restricts the model's ability to generalize to unseen cases. Data augmentation techniques could potentially mitigate this issue by artificially expanding the dataset and introducing greater variability. Moreover, the existing images in the dataset are of inconsistent or lower quality, further complicating feature extraction and pattern recognition during model training. These combined challenges — class imbalance, limited dataset size, and subpar image quality — significantly hinder the model's capacity to achieve higher accuracy and more robust performance metrics. Addressing these issues through improved data curation, augmentation, and potentially employing advanced model architectures may lead to better diagnostic outcomes in future iterations.

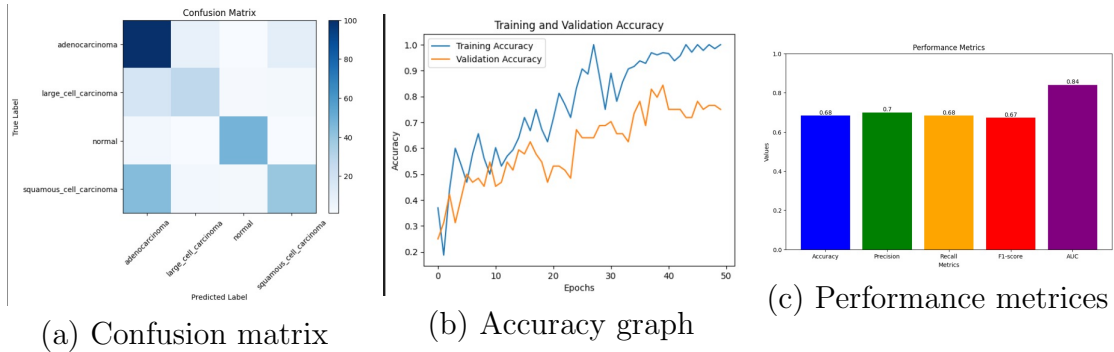


Figure 5.5: Results of Lung Cancer Model

# Chapter 6

## Conclusions

The Diagnosis AI project signifies a substantial advancement in the domain of automated disease diagnosis, integrating artificial intelligence (AI) and machine learning (ML) techniques to develop robust diagnostic solutions for critical conditions, including skin cancer, brain tumors, pneumonia, and lung cancer. By leveraging diverse medical imaging datasets and state-of-the-art algorithms, the project seeks to transform conventional disease detection methods, enhance diagnostic accuracy, and ultimately improve patient outcomes. The project adopts a comprehensive approach encompassing meticulous image preprocessing, advanced data augmentation strategies, and the design and optimization of deep learning architectures tailored for each disease category. These efforts have resulted in the development of high-performing models capable of rapid, precise, and reliable disease identification.

Furthermore, the project emphasizes the importance of addressing challenges such as class imbalance, data scarcity, and variability in image quality—factors that often hinder model generalization and clinical applicability. By employing techniques like transfer learning, feature extraction, and comparative model evaluation (including both deep learning and traditional machine learning classifiers), Diagnosis AI ensures that model development aligns closely with clinical objectives, such as minimizing false negatives and maintaining interpretability.

Ultimately, Diagnosis AI bridges the gap between cutting-edge technological innovation and real-world clinical practice. It lays the groundwork for a future where diagnostic processes are not only accurate and efficient but also accessible across diverse healthcare settings. This integration of AI into medical diagnostics has the potential to significantly streamline workflows, reduce diagnostic errors, and facilitate early disease detection, thereby contributing to improved healthcare delivery and patient care.

# Bibliography

- [1] World Cancer Research Fund. (2020). *Skin Cancer Statistics*. Retrieved from <https://www.wcrf.org/dietandcancer/cancer-trends/skin-cancer-statistics>. Accessed on March 30, 2020.
- [2] AW, K., TG, S. J., S., AA, M., & RS, B. (2021). *Techniques of Cutaneous Examination for the Detection of Skin Cancer*. PubMed. Accessed on April 10, 2021.
- [3] Mahmud, M. I., Mamun, M., & Abdelgawad, A. (2023). *A Deep Analysis of Brain Tumor Detection for MRI Images Using Deep Learning Networks*. Algorithms, MDPI. (Preprint).
- [4] Hany, M. (2020, August 20). *Chest CT-scan Images Dataset*. Kaggle. Retrieved from <https://www.kaggle.com/datasets/mohamedhanyyy/chest-ctscan-images>. Accessed on November 13, 2022.
- [5] Mamun, M., et al. (2023). *Lcdtcnn: Lung Cancer Diagnosis of CT Scan Images Using CNN Based Model*. In *10th International Conference on Signal Processing and Integrated Networks (SPIN)*. IEEE.
- [6] *Brain Tumour Detection Using Deep Learning*. IEEE Xplore. Retrieved from <https://ieeexplore.ieee.org/stamp/stamp.jsp?tp=arnumber=9445185>.
- [7] *A Deep Analysis of Brain Tumor Detection from MR Images Using Deep Learning Networks*. (2021). MDPI. Retrieved from <https://www.mdpi.com/1999-4893/16/4/176>.
- [8] He, K., Zhang, X., Ren, S., & Sun, J. (2015). *Deep Residual Learning for Image Recognition*. arXiv preprint arXiv:1512.03385.